Towards a dispersive determination of the η and η' transition form factors

Bastian Kubis[1,⋆]

[1] *Helmholtz-Institut für Strahlen- und Kernphysik (Theorie) and Bethe Center for Theoretical Physics, Universität Bonn, 53115 Bonn, Germany*

Abstract. We discuss status and prospects of a dispersive analysis of the η and η' transition form factors. Particular focus is put on the various pieces of experimental information that serve as input to such a calculation. These can help improve on the precision of an evaluation of the η and η' pole contributions to hadronic light-by-light scattering in the anomalous magnetic moment of the muon.

1 Hadronic light-by-light scattering and the anomalous magnetic moment of the muon

There is a by now long-standing discrepancy between the experimental determination of the anomalous magnetic moment of the muon as measured by the BNL E821 experiment [1], and its calculation within the Standard Model [2], with both experiment and theory affected by a comparable uncertainty. With two different proposals to further improve on the accuracy of the measurement well under way [3, 4], it is of utmost importance to also improve the accuracy of the theoretical Standard-Model prediction before a persistent discrepancy of potentially increased significance can be interpreted in terms of physics beyond the Standard Model.

The Standard-Model uncertainty is entirely dominated by hadronic contributions. While the dominant hadronic vacuum polarization can be expressed, via a dispersion relation, in terms of measurable $e^+e^- \to$ hadrons total cross sections, which therefore can be further improved upon by a strong experimental effort to determine many of the exclusive channels contributing therein with yet improved precision [5], the situation for the $\alpha_{\rm QED}$-suppressed hadronic light-by-light scattering is less straightforward, relying until recently to a much larger extent on modeling [6], with badly controlled errors.

This presentation is part of an effort to analyze also the hadronic light-by-light scattering tensor using dispersion theory [7, 8]. Dispersion theory makes maximal use of *analyticity* and *unitarity*, two fundamental consequences of relativistic quantum field theories that mathematically incorporate the principles of *causality* and *probability conservation*. The various (in principle infinitely many different) contributions to hadronic light-by-light scattering are organized in terms of their analytic structure, according to the cuts and poles in the different energy variables that are dictated by the above principles. This has the advantage that all contributions will be given in terms of on-shell form factors and scattering amplitudes, hence observables that can to a large extent again be related to experimentally accessible quantities [9]. An ordering principle will be to consider intermediate

⋆e-mail: kubis@hiskp.uni-bonn.de

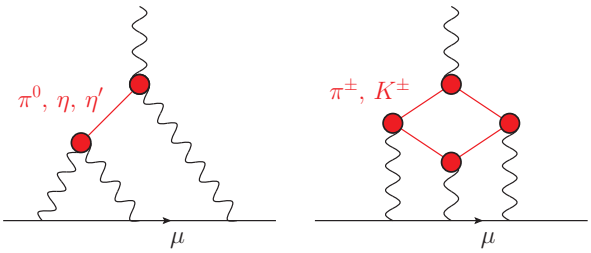

Figure 1. Dominant contributions to hadronic light-by-light scattering: pseudoscalar pole terms (left) and pion/kaon loop graphs (right).

states in terms of increasing masses, hence the lightest pseudoscalar pole terms (π^0, η, η') as well as pion–pion intermediate states are expected to give the largest individual contributions; see Fig. 1. In addition, all such form factors and scattering amplitudes can in turn also be analyzed using dispersion theory: they are reconstructed from their discontinuities or imaginary parts, whose most important contributions are determined by the leading hadronic intermediate states. One therefore interrelates a larger set of possible data, and often can avoid the direct use of amplitudes with leptons in the final state that are strongly suppressed by powers of the fine structure constant α_{QED}; see the discussion in Sect. 2.3. We will here concentrate on the transition form factors of the η and the η' that determine the corresponding pole terms; parallel efforts similar in style exist for the π^0 transition form factor [10–12] as well as for the pion loop including rescattering effects [13, 14].

2 Dispersion relation for the η and η' singly-virtual transition form factors

2.1 Definition, intermediate states

The $\eta^{(\prime)}$ transition form factor that describes the process $\eta^{(\prime)} \to \gamma^*\gamma^*$ is defined according to

$$\int \mathrm{d}^4x e^{iq_1x} i\langle 0|T\{j_\mu(x)j_\nu(0)|\eta^{(\prime)}(q_1+q_2)\rangle = -\epsilon_{\mu\nu\alpha\beta}q_1^\alpha q_2^\beta F_{\eta^{(\prime)}\gamma^*\gamma^*}(q_1^2,q_2^2)\,, \tag{1}$$

where

$$j_\mu = e\sum_f Q_f \bar{q}_f \gamma_\mu q_f \tag{2}$$

denotes the electromagnetic vector current for quarks of all flavors f, weighted with the respective electric quark charges Q_f. In order to write down dispersion relations in the two virtualities $q^2_{1/2}$, we first decompose the form factors in terms of isospin: while the neutral pion always needs to decay into one isovector and one isoscalar photon (vs), combined in both possible ways, the $\eta^{(\prime)}$ is given by the sum of two distinct contributions, an isovector–isovector (vv) and an isoscalar–isoscalar (ss) one,

$$F_{\eta^{(\prime)}\gamma^*\gamma^*}(q_1^2,q_2^2) = F_{vv}(q_1^2,q_2^2) + F_{ss}(q_1^2,q_2^2)\,, \qquad F_{\pi^0\gamma^*\gamma^*}(q_1^2,q_2^2) = F_{vs}(q_1^2,q_2^2) + F_{vs}(q_2^2,q_1^2)\,. \tag{3}$$

We need to identify the dominant intermediate states at low energies, where high precision is of paramount importance. These are depicted in Fig. 2. For the isovector photons, the most important intermediate state consists of a pair of charged pions, while for the isoscalar ones, three pions are the lightest option. The isovector dispersion relation will then express the transition form factor in

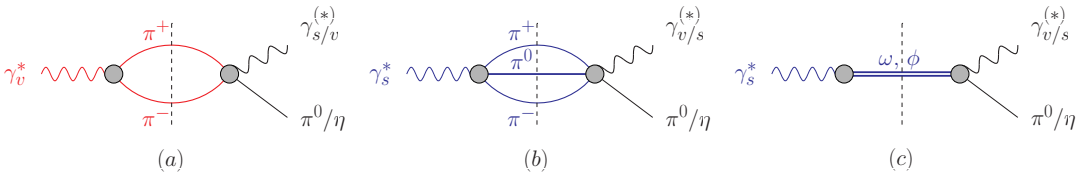

Figure 2. Leading intermediate hadronic states in π^0 and η transition form factors: (a) due to two pions for an isovector photon, (b) due to three pions for an isoscalar photon, (c) the three-pion intermediate state approximated by the lightest isoscalar vector resonances ω and ϕ.

terms of the product of the pion vector form factor $F_\pi^V(s)$ and the decay amplitude $\eta^{(\prime)} \to \pi^+\pi^-\gamma^{(*)}$ (the amplitude $\gamma^{(*)}\pi^0 \to \pi^+\pi^-$ in the case of the π^0)—this is what we will discuss in more detail below. The most general description of the three-pion intermediate state for the isoscalar photons, in contrast, would be a lot more complicated, and certain approximations at least for the transitions $3\pi \to \gamma^{(*)}\pi^0/\eta^{(\prime)}$ are almost unavoidable (see e.g. the corresponding discussion in Ref. [11]). Fortunately, the vector–isoscalar spectral function at low energies is strongly dominated by the narrow ω and ϕ resonances, see Fig. 2(c), such that a vector-meson-dominance (VMD) approximation is justified here to a large extent. In the context of the π^0, the corresponding $\omega \to \pi^0\gamma^*$ and $\phi \to \pi^0\gamma^*$ transition form factors have hence been treated dispersively [15–17] (see Ref. [18] for an extension even to the $J/\psi \to \pi^0\gamma^*$ transition), while a pure VMD description for $F_{ss}(q_1^2, q_2^2)$ was so far deemed sufficient for the $\eta^{(\prime)}$ transition form factors.

In the following, we will discuss how the different hadronic sub-amplitudes that are required as input to the unitarity relations can in turn be reconstructed based on dispersive methods.

2.2 Universality of final-state interactions, $\eta \to \pi^+\pi^-\gamma$

Final-state interactions between two strongly interacting particles as asymptotic states can be described in terms of form factors, which in turn can be linked to the properties of scattering amplitudes using analyticity and unitarity. As illustrated in Fig. 3, the unitarity relation for a pion form factor $F_J^I(s)$ of isospin I and angular momentum J reads

$$\operatorname{disc} F_J^I(s) = 2i \operatorname{Im} F_J^I(s) = 2i\, F_J^I(s) \times \theta(s - 4M_\pi^2) \times \sin\delta_J^I(s) e^{-i\delta_J^I(s)}\,, \tag{4}$$

from which one immediately deduces Watson's final-state theorem [19]: the form factor shares the phase $\delta_J^I(s)$ of the (elastic) scattering amplitude. The solution to Eq. (4) is obtained in terms of the

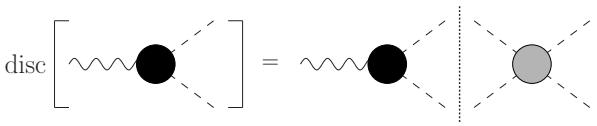

Figure 3. Graphical representation of the discontinuity relation for pion form factors. The black disc denotes the form factor, while the gray disc denotes the pion–pion scattering T-matrix, projected onto the appropriate partial wave.

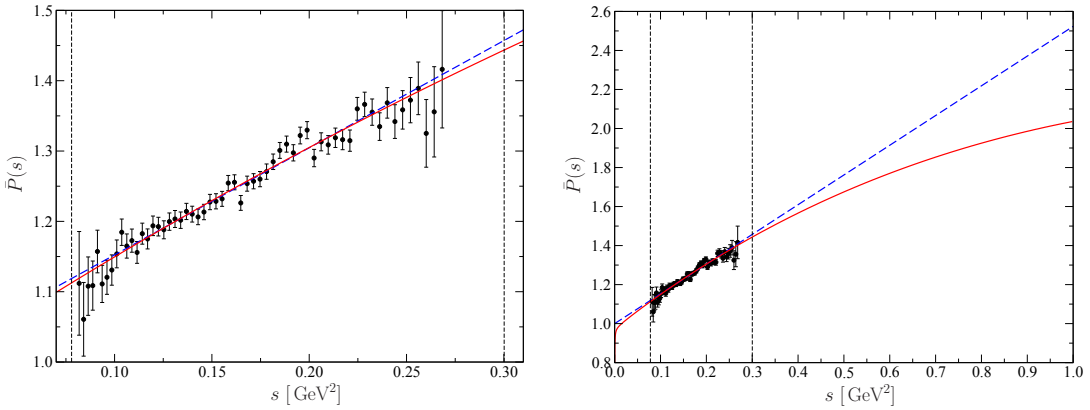

Figure 4. Left panel: representation of the decay distribution $\eta \to \pi^+\pi^-\gamma$ to allow for comparison to the polynomial $\bar{P}(s) = 1 + \alpha s$ (blue dashed curve). The full red curve includes the effects of a_2-exchange in addition; compare the discussion in Sect. 2.4. The vertical dashed lines denote the boundaries of phase space at $s = 4M_\pi^2$ and $s = M_\eta^2$. Right panel: the same distribution, extended up to $s = 1\,\text{GeV}^2$.

Omnès function $\Omega_J^I(s)$ [20],

$$F_J^I(s) = P_J^I(s)\Omega_J^I(s)\,, \quad \Omega_J^I(s) = \exp\left\{\frac{s}{\pi}\int_{4M_\pi^2}^{\infty} \mathrm{d}x \frac{\delta_J^I(x)}{x(x-s)}\right\}, \tag{5}$$

where $P_J^I(s)$ is a polynomial whose coefficients need to be determined by other methods, e.g. by matching to chiral perturbation theory near $s = 0$. The Omnès function is entirely given in terms of the appropriate pion–pion phase shift, which is particularly useful as we today have excellent information on pion–pion scattering at our disposal [21–24]. The pion vector form factor $F_\pi^V(s)$ as extracted from $\tau^- \to \pi^-\pi^0\nu_\tau$ decays, e.g., can be described very accurately by a representation (5) up to $\sqrt{s} = 1\,\text{GeV}$, employing a *linear* polynomial $R(s) \equiv P_1^1(s) = 1 + \alpha_V s$—at higher energies, the nonlinear effects of higher, inelastic (ρ', ρ'') resonances become important [25]. The slope parameter α_V therein is relatively small, $\alpha_V \sim 0.1\,\text{GeV}^{-2}$. For the pion vector form factor as measured in $e^+e^- \to \pi^+\pi^-$, the isospin-violating mixing effect with the ω-meson needs to be taken into account, see e.g. the extensive recent discussion in Ref. [26].

The power of the universality of final-state interactions lies in the fact that an Omnès representation similar to the one for the vector form factor will apply everywhere where two pions are produced from a point source in a relative P-wave; the process-dependence can be reduced to the coefficients of the multiplicative polynomial. It was pointed out that such a representation can in particular be used for the decays $\eta^{(\prime)} \to \pi^+\pi^-\gamma$ [27]: they are driven by the chiral anomaly and require the pion pair to be in an odd partial wave, hence the assumption of dominance by the P-wave $f_1(s)$ is entirely justified. For the decay of the η, an ansatz with a linear polynomial,

$$f_1(s) = A(1 + \alpha s)\Omega_1^1(s)\,, \tag{6}$$

was shown to be sufficient to describe the data in the physical decay region [28, 29], however, with one important difference to the vector form factor: α turns out to be large, $\alpha \sim 1.5\,\text{GeV}^{-2}$ [29, 30]; see Fig. 4.

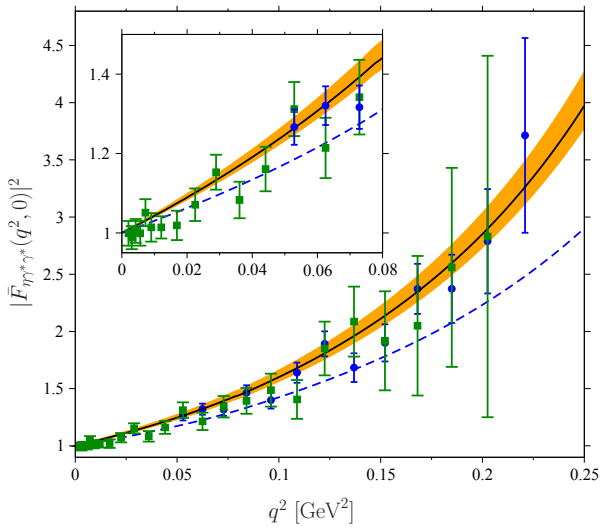

Figure 5. Comparison of the dispersive prediction for $|\bar{F}_{\eta\gamma^*\gamma^*}(q^2,0)|^2$ to data from the A2 [31] (green) and NA60 [34] (blue) collaborations. Figure courtesy of C. Hanhart.

2.3 Dispersive prediction for $\eta \to \ell^+\ell^-\gamma$

With the input to the isovector dispersion relation fixed, we can therefore calculate the singly-virtual η transition form factor: employing a once-subtracted dispersion relation for the normalized form factor $\bar{F}_{\eta\gamma^*\gamma^*}(q^2,0) = F_{\eta\gamma^*\gamma^*}(q^2,0)/F_{\eta\gamma^*\gamma^*}(0,0)$, one finds [25]

$$\bar{F}_{\eta\gamma^*\gamma^*}(q^2,0) = 1 + \frac{e\,q^2}{96\pi^2 A^\eta_{\gamma\gamma}} \int_{4M_\pi^2}^{\infty} \frac{\mathrm{d}x}{x-q^2}\left(1-\frac{4M_\pi^2}{x}\right)^{3/2} F_\pi^{V*}(x) f_1(x) + \Delta F^{I=0}_{\eta\gamma^*\gamma^*}(q^2,0)\,, \tag{7}$$

where $A^\eta_{\gamma\gamma}$ is related to the $\eta \to 2\gamma$ real-photon decay width, and the last term denotes the (small) isoscalar contribution; see Refs. [25, 30] for details. The resulting prediction includes the propagated uncertainties both from the experimental input employed and due to the high-energy continuation of the dispersion integral; see Ref. [25] for a detailed discussion. It can be compared to the experimental data on the decays $\eta \to \ell^+\ell^-\gamma$, which have been obtained both for the electron–positron [31, 32] and the dimuon [33, 34] final states. In Fig. 5, we observe one of the main strengths of the dispersive approach: by fixing the input to the singly-radiative decay $\eta \to \pi^+\pi^-\gamma$ (with the decay rate scaling according to $\propto \alpha_{\mathrm{QED}}$), we gain a huge statistical advantage over the direct measurements of $\eta \to \ell^+\ell^-\gamma$ (rate $\propto \alpha^3_{\mathrm{QED}}$). A direct measurement of the transition form factor of comparable precision to the theoretical calculation based on dispersion relations will be enormously difficult.

2.4 Left-hand cuts

We have remarked above that the interpretation of the polynomial parameters multiplying the universal Omnès function has to be obtained case by case, and observed that the slope parameters α_V for the pion vector form factor and α in the $\eta \to \pi^+\pi^-\gamma$ decay are very different. While α_V can consistently be described as the low-energy tail of higher resonances in the region $1\,\mathrm{GeV} \lesssim \sqrt{s} \lesssim 2\,\mathrm{GeV}$, such an interpretation seems implausible for the $\eta \to \pi^+\pi^-\gamma$ decay. Furthermore, it is known that a linear

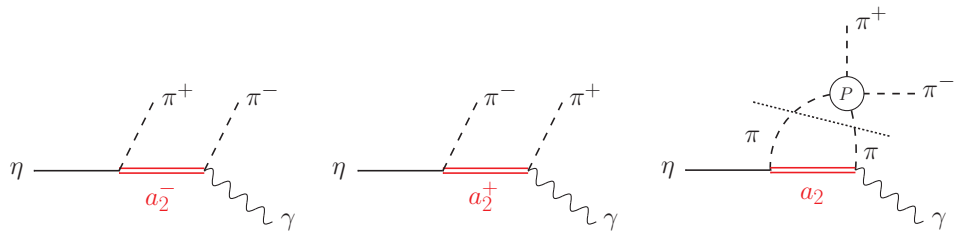

Figure 6. a_2 contributions to $\eta \to \pi^+\pi^-\gamma$, both at tree level and including pion–pion P-wave rescattering. The combination of both is required to preserve the final-state theorem.

polynomial $P(s)$ can only be a low-energy approximation: with the pion–pion P-wave Omnès function dropping like $1/s$ for large energies, the polynomial multiplying it should rather approach a constant asymptotically. Given that the dispersion integral to calculate the transition form factor formally extends to infinity, deviations from the linear rise in $P(s)$ may become important. It is therefore crucial to search for opportunities to investigate the amplitude $f_1(s)$ outside the relatively narrow η decay region.

One remarkable property of the amplitude (6) is the fact that it displays a zero for negative values of s at $s = -1/\alpha \approx -0.66\,\text{GeV}^2$, which therefore occurs at rather low energies. This kinematic configuration can be tested in the crossed process $\gamma\pi^- \to \pi^-\eta$, which can be investigated experimentally in a Primakoff reaction, i.e. the scattering of highly energetic charged pions in the strong Coulomb field of a heavy nucleus, e.g. at COMPASS; see Ref. [35] for an overview of the COMPASS Primakoff program and Ref. [36] for a first attempt to access the $\gamma\pi^- \to \pi^-\eta$ reaction. The zero would then occur in the angular distribution at fixed energies in the crossed center-of-mass system. In order to judge how reliable such a prediction is, we need to consider the possible effects of nontrivial $\pi\eta$ dynamics—something that has been entirely neglected in the discussion of the decay $\eta \to \pi^+\pi^-\gamma$ so far. A $\pi\eta$ S-wave is forbidden in this anomalous process. The P-wave is of exotic quantum numbers, $J^{PC} = 1^{-+}$, i.e. there are no resonances possible in a quark model of mesons, and no resonant states have been identified unambiguously so far [37, 38]; hence the P-wave is expected to be very weak at low energies. The first resonance to occur in $\gamma\pi^- \to \pi^-\eta$ is therefore the D-wave $a_2(1320)$. At the same time, it provides the dominant left-hand-cut contribution to the decay $\eta \to \pi^+\pi^-\gamma$ that has not been considered so far: a dispersion relation including the effects of a_2-exchange, see Fig. 6, is more complicated than the form factor relation (4), and requires a more complicated solution; for details, see Ref. [30]. There also the predictions for the Primakoff reaction $\gamma\pi^- \to \pi^-\eta$ are discussed: the zero of the simple amplitude representation (6) partially survives in the form of a strong amplitude suppression in backward direction in the energy region between threshold and the a_2 resonance, that can be explained as a P-D-wave interference effect. Here we only discuss the compatibility of this more refined model with the decay data: if the very precise data on $\eta \to \pi^+\pi^-\gamma$ by the KLOE collaboration [29] were already accurately described by the simpler amplitude of the form $P(s) \times \Omega_1^1(s)$, is this accuracy preserved when including a_2 effects? The answer is shown in Fig. 4: the left-hand cut induces a curvature in $P(s)$ that has only very small effects in the decay region, resulting in a data fit of equal quality; however, plotted over a larger energy region, it becomes clear that the effect on the dispersion integrals for the η transition form factor is nonnegligible. If one evaluates a sum rule for the slope of the form factor at $q^2 = 0$ that is easily obtained from Eq. (7), one finds that the a_2 effects reduce this slope by 7–8%.

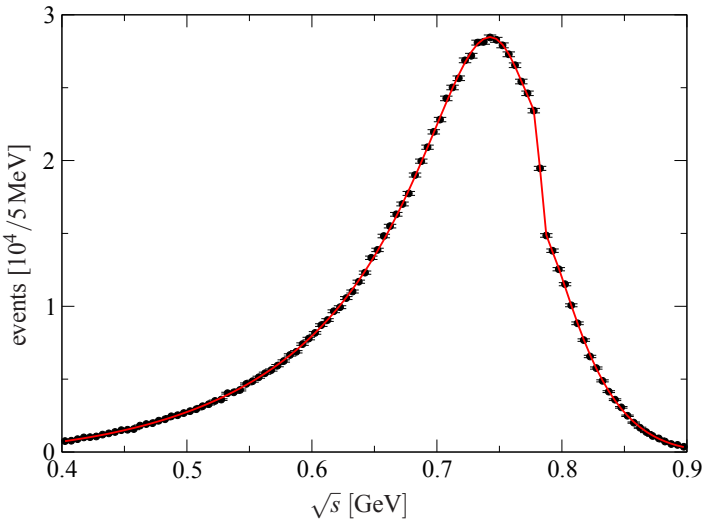

Figure 7. Differential decay rate $\mathrm{d}\Gamma(\eta' \to \pi^+\pi^-\gamma)/\mathrm{d}\sqrt{s}$. Pseudo-data generated according to preliminary BESIII results [40] is compared to the best fit according to Eq. (8). Figure taken from Ref. [26].

2.5 $\eta' \to \pi^+\pi^-\gamma$ and η' transition form factor

All the steps discussed in the previous subsections can in principle be carried over to an analysis of the η' transition form factor in a straightforward manner. While old data on $\eta' \to \pi^+\pi^-\gamma$ by the Crystal Barrel Collaboration [39] were not precise enough for an advanced analysis, a new, forthcoming measurement by BESIII [40] is in certain ways even more conclusive than the η decay data, as the larger phase space of the η' decay allows one to see deviations from the assumption of a linear polynomial much more clearly. It has been demonstrated in Ref. [30] that, despite the occurrence of a left-hand cut, in fact the ratio $f_1(s)/\Omega_1^1(s)$ in the model including the a_2 can be approximated very accurately by a *quadratic* polynomial within the physical decay region, i.e. for $4M_\pi^2 \le s \le M_{\eta'}^2$. The preliminary BESIII data [40] demonstrate the need of such a quadratic term to very high significance; moreover, they are so precise that even the isospin-breaking ρ–ω-mixing effect is clearly discernible (see Ref. [26] for details on how to extract the mixing strength and subsequently the partial width $\Gamma(\omega \to \pi^+\pi^-)$ from this decay). The full representation of the $\eta' \to \pi^+\pi^-\gamma$ P-wave amplitude is therefore of the form [26]

$$f_1(s) = \left[A(1 + \alpha s + \beta s^2) + \frac{\kappa_2}{m_\omega^2 - s - i m_\omega \Gamma_\omega}\right] \times \Omega_1^1(s)\,. \tag{8}$$

The fit to pseudo-data generated according to preliminary results is shown in Fig. 7. The leading left-hand-cut contribution provided by a_2-exchange gives an estimate of the parameter $\beta = (-1.0 \pm 0.1)\,\mathrm{GeV}^{-4}$ [30], which yields the correct sign and order of magnitude, but is somewhat larger than what the new data suggest [26].

The combination of the very precise representation of the $\eta' \to \pi^+\pi^-\gamma$ decay amplitude as well as the pion vector form factor then once more yields a dispersive prediction of the isovector part of the η' (singly-virtual) transition form factor according to the analogous formula to Eq. (7) [41]. In comparison to the η form factor, the isoscalar contribution is larger; however, this can be modeled well using the vector-meson-dominance assumption, with the necessary coupling constants extracted from

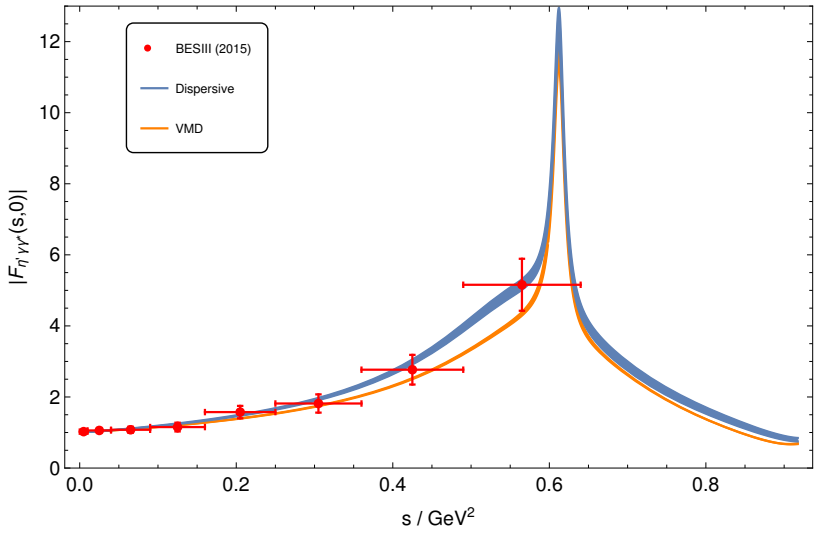

Figure 8. Dispersion-theoretical prediction for the singly-virtual η' transition form factor (blue band), compared to a vector-meson-dominance model (orange), as well as the data points taken by the BESIII collaboration [42]. Figure courtesy of S. Holz.

the partial decay widths for $\eta' \to \omega\gamma$ and $\omega \to \ell^+\ell^-$ as well as $\phi \to \eta'\gamma$ and $\phi \to \ell^+\ell^-$. The combined prediction for the singly-virtual η' transition form factor is shown in Fig. 8 as the blue band [41]. Both the broad resonance shape due to the ρ enhancement and the narrow ω peak are clearly visible. The error band comprises the propagated uncertainties due to different pion form factor data sets, different pion–pion scattering phase shifts, and different assumptions on the high-energy continuation of the input to the dispersion integral. However, despite these uncertainties we still note significant deviations of the dispersive prediction from a pure VMD model (with a simple finite-width ρ^0 pole as the isovector contribution), which is due to the much more sophisticated treatment of the two-pion cut contribution. The available data on $\eta' \to e^+e^-\gamma$ from BESIII [42] are not yet precise enough to differentiate between the two theoretical curves; new data also from other laboratories are eagerly awaited.

3 Towards a description of the doubly-virtual $\eta^{(\prime)}$ transition form factors

In the previous section, we have discussed in detail that dispersion theory provides a very accurate description of the singly-virtual $\eta^{(\prime)}$ transition form factors, based on high-precision experimental data that allows us to fix a small number of free polynomial parameters in the various dispersive amplitude representations. We have confined our discussion to experimental tests of the timelike form factors that can be measured in the decays $\eta^{(\prime)} \to \ell^+\ell^-\gamma$; we wish to emphasize that as the form factors by construction have the correct analytic structure, they can be analytically continued into the spacelike region without difficulties, i.e. Eq. (7) is easily evaluated for $q^2 < 0$. We expect this description to be reliable in a similar range of $|q^2|$ as the timelike momenta that enter the description of the spectral function, $-q^2 \lesssim 1\,\text{GeV}^2$; compare the related discussion of the π^0 transition form factor for spacelike arguments in Ref. [11].

The light-by-light loop integral that determines the pseudoscalar pole contributions to the anomalous magnetic moment of the muon, however, also requires the doubly-virtual transition form factors, see Fig. 1, hence the next challenge is to extend the formalism presented above to this more complicated case.

3.1 Testing factorization in $e^+e^- \to \eta\pi^+\pi^-$

One possible reaction in which the doubly-virtual (timelike) η transition form factor is directly accessible experimentally is obviously $e^+e^- \to \eta e^+e^-$. However, this process is strongly suppressed in the fine structure constant, and in the spirit of the preceding, we point to the much more promising possibility to investigate $e^+e^- \to \eta\pi^+\pi^-$ instead, thus beating the suppression by α_{QED}^2, and subsequently using a dispersion relation to reconstruct the dependence on the second (outgoing) photon's virtuality by means of the dominant $\pi^+\pi^-$ intermediate state.

One assumption frequently employed in the description of doubly-virtual transition form factors at low-to-moderate energies is the one of factorization: the dependence on the two virtualities is simplified into the product of two functions of a single variable each. For the example of the isovector–isovector contribution to the η transition form factor, the assumption for the normalized function $\bar{F}_{vv}(q_1^2, q_2^2) = F_{vv}(q_1^2, q_2^2)/F_{vv}(0,0)$ reads

$$\bar{F}_{vv}(q_1^2, q_2^2) \overset{?!}{=} \bar{F}_{vv}(q_1^2, 0) \times \bar{F}_{vv}(0, q_2^2) = \bar{F}_{vv}(q_1^2, 0) \times \bar{F}_{vv}(q_2^2, 0)\,. \tag{9}$$

We can test this factorization hypothesis also in $e^+e^- \to \eta\pi^+\pi^-$ [43]. Denoting the $\pi^+\pi^-$ squared invariant mass by $s_{\pi\pi}$ and the dilepton/the $\eta\pi^+\pi^-$ invariant mass squared by Q_2^2, it translates into

$$F_{\eta\pi\pi\gamma^*}(s_{\pi\pi}, Q_2^2) \overset{?!}{=} F_{\eta\pi\pi\gamma}(s_{\pi\pi}) \times F_{\eta\gamma\gamma^*}(Q_2^2)\,. \tag{10}$$

In other words: for fixed Q_2^2, factorization predicts the same dependence on $s_{\pi\pi}$ as observed in the real-photon case, i.e. in the decay $\eta \to \pi^+\pi^-\gamma$. Our strategy is therefore as follows: we allow for a similar functional form for $F_{\eta\pi\pi\gamma}(s_{\pi\pi})$ as in Sects. 2.2 and 2.4, i.e. an Omnès function multiplied with a linear polynomial in the one case, and including the effects of left-hand cuts due to a_2-exchange in the other. The subtraction constants can then be fitted to data and subsequently compared to the real-photon decay amplitude. As Q_2^2 is necessarily large—the reaction threshold is around $\sqrt{Q_2^2} = 0.83\,\text{GeV}$, and the cross section is dominated by the ρ' or $\rho(1450)$ resonance—we for the moment simply parametrize $F_{\eta\gamma\gamma^*}(Q_2^2)$ by a sum of two Breit–Wigner functions [for the $\rho(770)$ and the $\rho(1450)$].

Unfortunately, the BaBar data [44] that we have analyzed for this purpose are not truly doubly differential in $s_{\pi\pi}$ and Q_2^2: only the total cross section $\sigma_{\text{tot}}(Q_2^2)$ as well as the $\pi\pi$ spectrum $d\Gamma/d\sqrt{s_{\pi\pi}}$, integrated over $1\,\text{GeV} \leq \sqrt{Q_2^2} \leq 4.5\,\text{GeV}$, are available. The best fit to the data is shown in Fig. 9. We find that fitting a linear polynomial in $F_{\eta\pi\pi\gamma}(s_{\pi\pi})$ leads to polynomial parameters that are incompatible with the ones found in $\eta \to \pi^+\pi^-\gamma$, hence seemingly pointing towards a large violation of the factorization assumption. In contrast, preliminary results including effects of a_2-exchange indicate that such a violation is much attenuated in this case [43].

3.2 Double spectral function based on $\eta' \to \pi^+\pi^-\pi^+\pi^-$

We have emphasized repeatedly how it is advantageous to use hadronic amplitudes, which can be measured much more precisely due to the statistical advantage of lack of suppression in α_{QED}, as input to dispersion relations instead of measuring radiative amplitudes directly; therefore, we have based

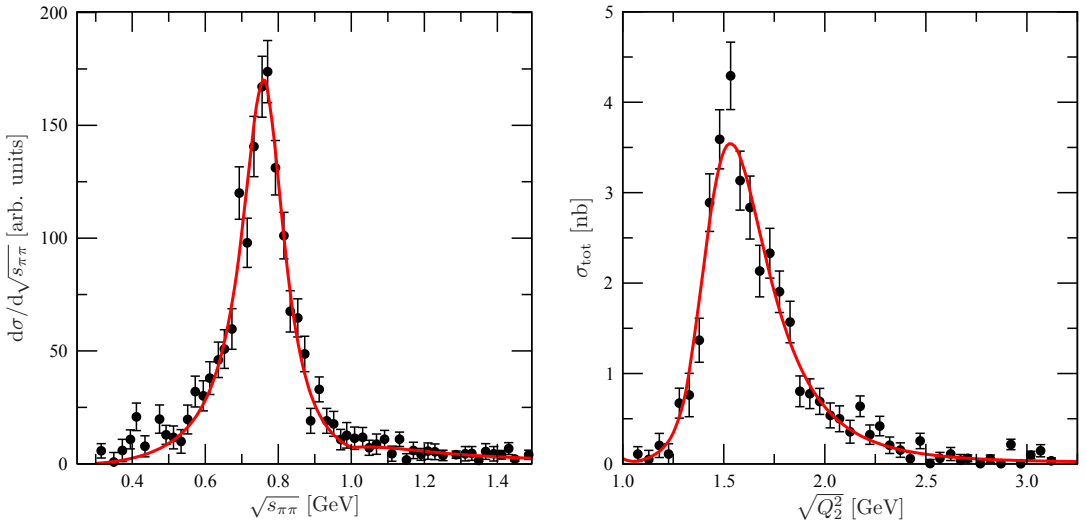

Figure 9. Result of the best fit to both the $\pi\pi$ spectrum (left panel) and the total cross section (right panel) for the reaction $e^+e^- \to \eta\pi^+\pi^-$. The data are from Ref. [44]. Figure taken from Ref. [43].

predictions for $\eta^{(\prime)} \to \ell^+\ell^-\gamma$ on precision data for $\eta^{(\prime)} \to \pi^+\pi^-\gamma$. In order to calculate the doubly-virtual transition form factor (or, more precisely, the isovector–isovector contribution therein), we may therefore consider going even one step further and base the construction of a double spectral function on a model for the purely hadronic decay $\eta' \to \pi^+\pi^-\pi^+\pi^-$. This decay has been analyzed in Ref. [45], combining the chiral expansion (the leading decay amplitude only occurs at $O(p^6)$) with vector-meson resonance saturation of the low-energy constants involved. It was found that the (virtual) decay chain $\eta' \to 2\rho^0 \to 2(\pi^+\pi^-)$ entirely dominates the reaction. The prediction for the branching fraction, $\mathcal{B}(\eta' \to \pi^+\pi^-\pi^+\pi^-) = (10 \pm 3) \times 10^{-5}$ [45], has subsequently been confirmed by BESIII [46] with a smaller uncertainty,

$$\mathcal{B}(\eta' \to \pi^+\pi^-\pi^+\pi^-) = (8.7 \pm 0.7 \pm 0.6) \times 10^{-5}\,, \tag{11}$$

hence a theoretical refinement of the amplitude analysis is in order.

However, even based on the preliminary model of Ref. [45], we can attempt to assess the size of nonfactorizing contributions to the doubly-virtual η' transition form factor, see Fig. 10, by combining $\pi^+\pi^-$ pairs into virtual photons in the sense of a dispersion relation: it naturally yields a (dominant) factorizing term that closely resembles a VMD model, see the left diagram in Fig. 10, and a nonfactorizing one, where the charged pions stemming from different intermediate ρ^0 resonances are recombined [Fig. 10 (right)]. First steps towards such an investigation indicate that these nonfactorizing terms are small [47].

4 Summary, and a wish list for improved experimental input

We have shown that dispersion relations allow for high-precision predictions of the singly-virtual $\eta^{(\prime)}$ transition form factors, based on high-precision data for $\eta \to \pi^+\pi^-\gamma$ by KLOE [29] and for $\eta' \to \pi^+\pi^-\gamma$ by BESIII [40], as well as data on the pion vector form factor that is known to excellent precision, largely due to the strong experimental campaign to reduce the error on hadronic vacuum polarization in the muon's anomalous magnetic moment [48–53].

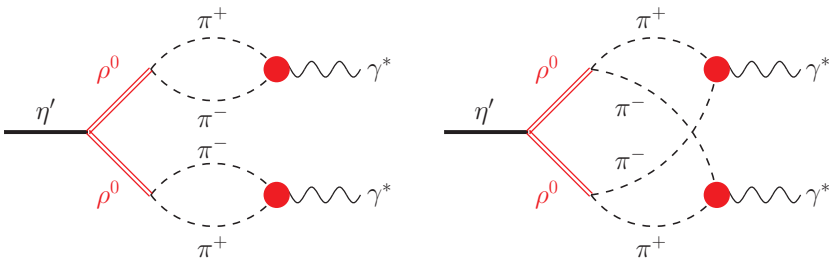

Figure 10. Factorizing (left) and nonfactorizing (right) contributions to the doubly-virtual η' transition form factor, based on a vector-meson-dominance model for the amplitude $\eta' \to \pi^+\pi^-\pi^+\pi^-$.

The following additional pieces of experimental information will help improve these model-independent, data-driven determinations, largely with the aim to extend the existing analysis to the doubly-virtual case.

1. A measurement of the Primakoff-type process $\gamma\pi^- \to \pi^-\eta$ allows for better constrained high-energy input to the existing analysis.

2. More differential data on $e^+e^- \to \eta\pi^+\pi^-$, i.e., measurements of the dipion distribution for smaller bins in the total e^+e^- energy, or even $\eta\pi^+\pi^-$ Dalitz plot distributions, would be extremely helpful to understand deviations from the factorization hypothesis for the doubly-virtual form factor, which is known to be invalid at high energies.

3. More detailed, differential decay data on $\eta' \to \pi^+\pi^-\pi^+\pi^-$ may allow us to construct a double spectral function for the doubly-virtual η' transition form factor; the precise form in which such differential data for a four-body decay ought to be analyzed should be developed in close collaboration between experimentalists and theorists.

4. Finally, given the fantastic precision of the upcoming BESIII data on $\eta' \to \pi^+\pi^-\gamma$, a direct measurement of $\eta' \to \pi^+\pi^-e^+e^-$ with good precision may be feasible.

The combination of further theoretical development along the lines sketched above, and improved experimental input for such a data-driven approach will therefore pave the way to a determination of the $\eta^{(\prime)}$ pole contributions to hadronic light-by-light scattering with controlled uncertainties.

Acknowledgements I would like to thank the organizers of the *KLOE-2 Workshop on e^+e^- collider physics at 1 GeV* for the invitation to this exciting workshop, and Christoph Hanhart for useful comments on this writeup. This research is supported in part by the DFG and the NSFC through funds provided to the Sino–German CRC 110 “Symmetries and the Emergence of Structure in QCD” (NSFC Grant No. 11621131001, DFG Grant No. TRR110).

References

[1] G. W. Bennett *et al.* [Muon $g-2$ Collaboration], Phys. Rev. D **73**, 072003 (2006)
[2] F. Jegerlehner and A. Nyffeler, Phys. Rept. **477**, 1 (2009)
[3] J. Grange *et al.* [Muon $g-2$ Collaboration], arXiv:1501.06858 [physics.ins-det]
[4] N. Saito [J-PARC $g-2$/EDM Collaboration], AIP Conf. Proc. **1467**, 45 (2012)

[5] T. Blum, A. Denig, I. Logashenko, E. de Rafael, B. Lee Roberts, T. Teubner and G. Venanzoni, arXiv:1311.2198 [hep-ph]
[6] J. Prades, E. de Rafael and A. Vainshtein, Adv. Ser. Direct. High Energy Phys. **20**, 303 (2009)
[7] G. Colangelo, M. Hoferichter, M. Procura and P. Stoffer, JHEP **1409**, 091 (2014)
[8] G. Colangelo, M. Hoferichter, M. Procura and P. Stoffer, JHEP **1509**, 074 (2015)
[9] G. Colangelo, M. Hoferichter, B. Kubis, M. Procura and P. Stoffer, Phys. Lett. B **738**, 6 (2014)
[10] M. Hoferichter, B. Kubis and D. Sakkas, Phys. Rev. D **86**, 116009 (2012)
[11] M. Hoferichter, B. Kubis, S. Leupold, F. Niecknig and S. P. Schneider, Eur. Phys. J. C **74**, 3180 (2014)
[12] S. Leupold *et al.*, these proceedings
[13] G. Colangelo, M. Hoferichter, M. Procura and P. Stoffer, arXiv:1701.06554 [hep-ph]
[14] M. Procura *et al.*, these proceedings
[15] F. Niecknig, B. Kubis and S. P. Schneider, Eur. Phys. J. C **72**, 2014 (2012)
[16] S. P. Schneider, B. Kubis and F. Niecknig, Phys. Rev. D **86**, 054013 (2012)
[17] I. V. Danilkin, C. Fernández-Ramírez, P. Guo, V. Mathieu, D. Schott, M. Shi and A. P. Szczepaniak, Phys. Rev. D **91**, 094029 (2015)
[18] B. Kubis and F. Niecknig, Phys. Rev. D **91**, 036004 (2015)
[19] K. M. Watson, Phys. Rev. **95**, 228 (1954)
[20] R. Omnès, Nuovo Cim. **8**, 316 (1958)
[21] B. Ananthanarayan, G. Colangelo, J. Gasser and H. Leutwyler, Phys. Rept. **353**, 207 (2001)
[22] G. Colangelo, J. Gasser and H. Leutwyler, Nucl. Phys. B **603**, 125 (2001)
[23] R. García-Martín, R. Kamiński, J. R. Peláez, J. Ruiz de Elvira and F. J. Ynduráin, Phys. Rev. D **83**, 074004 (2011)
[24] I. Caprini, G. Colangelo, and H. Leutwyler, Eur. Phys. J. C **72**, 1860 (2012)
[25] C. Hanhart, A. Kupść, U.-G. Meißner, F. Stollenwerk and A. Wirzba, Eur. Phys. J. C **73**, 2668 (2013) [Erratum: Eur. Phys. J. C **75**, 242 (2015)]
[26] C. Hanhart, S. Holz, B. Kubis, A. Kupść, A. Wirzba and C. W. Xiao, Eur. Phys. J. C **77**, 98 (2017)
[27] F. Stollenwerk, C. Hanhart, A. Kupść, U.-G. Meißner and A. Wirzba, Phys. Lett. B **707**, 184 (2012)
[28] P. Adlarson *et al.* [WASA-at-COSY Collaboration], Phys. Lett. B **707**, 243 (2012)
[29] D. Babusci *et al.* [KLOE Collaboration], Phys. Lett. B **718**, 910 (2013)
[30] B. Kubis and J. Plenter, Eur. Phys. J. C **75**, 283 (2015)
[31] P. Aguar-Bartolome *et al.* [A2 Collaboration], Phys. Rev. C **89**, 044608 (2014)
[32] P. Adlarson *et al.*, arXiv:1609.04503 [hep-ex]
[33] R. Arnaldi *et al.* [NA60 Collaboration], Phys. Lett. B **677**, 260 (2009)
[34] R. Arnaldi *et al.* [NA60 Collaboration], Phys. Lett. B **757**, 437 (2016)
[35] N. Kaiser and J. M. Friedrich, Eur. Phys. J. A **36**, 181 (2008)
[36] E. Altenbach, *Diploma thesis* (University of Bonn, 2016)
[37] C. Adolph *et al.* [COMPASS Collaboration], Phys. Lett. B **740**, 303 (2015)
[38] D. Schott [CLAS Collaboration], PoS **Confinement X**, 106 (2012)
[39] A. Abele *et al.* [Crystal Barrel Collaboration], Phys. Lett. B **402**, 195 (1997)
[40] S.-s. Fang [BESIII Collaboration], PoS **CD 15**, 032 (2016)
[41] S. Holz, *Bachelor thesis* (University of Bonn, 2016)

[42] M. Ablikim *et al.* [BESIII Collaboration], Phys. Rev. D **92**, 012001 (2015)
[43] C. W. Xiao, T. Dato, C. Hanhart, B. Kubis, U.-G. Meißner and A. Wirzba, arXiv:1509.02194 [hep-ph]
[44] B. Aubert *et al.* [BaBar Collaboration], Phys. Rev. D **76**, 092005 (2007) [Erratum: Phys. Rev. D **77**, 119902 (2008)]
[45] F.-K. Guo, B. Kubis and A. Wirzba, Phys. Rev. D **85**, 014014 (2012)
[46] M. Ablikim *et al.* [BESIII Collaboration], Phys. Rev. Lett. **112**, 251801 (2014) [Addendum: Phys. Rev. Lett. **113**, 039903 (2014)]
[47] T. Dato, *Master thesis* (University of Bonn, 2016)
[48] M. N. Achasov *et al.*, J. Exp. Theor. Phys. **103**, 380 (2006) [Zh. Eksp. Teor. Fiz. **130**, 437 (2006)]
[49] R. R. Akhmetshin *et al.* [CMD-2 Collaboration], Phys. Lett. B **648**, 28 (2007)
[50] B. Aubert *et al.* [BaBar Collaboration], Phys. Rev. Lett. **103**, 231801 (2009)
[51] F. Ambrosino *et al.* [KLOE Collaboration], Phys. Lett. B **700**, 102 (2011)
[52] D. Babusci *et al.* [KLOE Collaboration], Phys. Lett. B **720**, 336 (2013)
[53] M. Ablikim *et al.* [BESIII Collaboration], Phys. Lett. B **753**, 629 (2016)